Acta Crystallographica Section B
**Structural Science**
ISSN 0108-7681

# $N^6$-Substituted 2-amino-4-chloro-5-formylpyrimidines: puckered *versus* planar pyrimidine rings, and hydrogen-bonded aggregation in zero, one, two and three dimensions

**Justo Cobo,[a] Jorge Trilleras,[b] Jairo Quiroga,[b] Antonio Marchal,[a] Manuel Nogueras,[a] John N. Low[c] and Christopher Glidewell[d]***

[a]Departamento de Química Inorgánica y Orgánica, Universidad de Jaén, 23071 Jaén, Spain, [b]Grupo de Investigación de Compuestos Heterocíclicos, Departamento de Química, Universidad de Valle, AA 25360 Cali, Colombia, [c]Department of Chemistry, University of Aberdeen, Meston Walk, Old Aberdeen AB24 3UE, Scotland, and [d]School of Chemistry, University of St Andrews, St Andrews, Fife KY16 9ST, Scotland

Correspondence e-mail: cg@st-andrews.ac.uk

Received 19 April 2008
Accepted 30 June 2008

The structures of 12 new $N^6$-substituted 2-amino-4-chloro-5-formylpyrimidines, where the $N^6$ substituent is of the type NH*R* or N$R^1R^2$, have been determined. The intramolecular dimensions provide strong evidence for the development of polarized, charge-separated molecular-electronic structures, with the positive charge delocalized over the two exocyclic amino N atoms and with negative charge on the formyl O atom. This polarization appears to be independent of the significant puckering, in seven of the compounds, of the pyrimidine rings from planarity towards boat, twist-boat or screw-boat conformations. In 11 of the compounds studied here, N—H···N hydrogen bonds link pairs of molecules into centrosymmetric $R_2^2(8)$ dimer units, and their overall crystal structures are determined by the patterns of hydrogen bonds by which these units are further linked. Examples are reported in which no further hydrogen bonding occurs; in which the $R_2^2(8)$ dimers are linked into chains of rings, or into sheets; and in which sheets are formed by the $\pi$-stacking of hydrogen-bonded chains of rings. In the sole structure lacking the $R_2^2(8)$ dimer motif, N—H···O and N—H···N hydrogen bonds cooperate to generate a three-dimensional framework structure.

## 1. Introduction

5-Nitrosopyrimidines in which there is a primary amino substituent in the 6-position, adjacent to the nitrosyl group, generally form intramolecular N—H···O hydrogen bonds (*A*; see Scheme 1; Low *et al.*, 1997, 1999, 2000; Quesada *et al.*, 2002, 2004; Melguizo *et al.*, 2003) to generate an *S*(6) motif (Bernstein *et al.*, 1995). Such pyrimidines are therefore isoelectronic and approximately isosteric with purines (*B*) and they can, in some instances, mimic the biological actions of purines. Thus, for example, the benzyloxy derivative (*A*; *X* = $NH_2$, *Y* = $PhCH_2O$, *Z* = H) is a more potent *in vitro* inhibitor (Chae *et al.*, 1995) of the human DNA-repair protein O-alkylguanine-DNA-transferase than the prototype inhibitor (*B*; *X* = $NH_2$, *Y* = $PhCH_2O$, *Z* = H; Friedman *et al.*, 1998; see Scheme 1).

When the substituent *X* in a nitrosopyrimidine of type (*A*) is an amino function, the bond distances provide evidence for very marked polarization of the molecular-electronic structure, leading to the development of a marked negative charge at the nitrosyl group (*C*). This in turn can lead, in cases where the substituent *R* carries an unionized carboxylic acid function, to the formation of very short intermolecular O—H···O hydrogen bonds where the nitrosyl O atom acts as the acceptor and where the O···O distances are no more than 2.50 Å, and sometimes somewhat less (Low *et al.*, 1997, 1999, 2000). A combination of database and modelling studies

confirmed the generality of these phenomena in C-nitroso compounds of this general type (Low *et al.*, 2000).

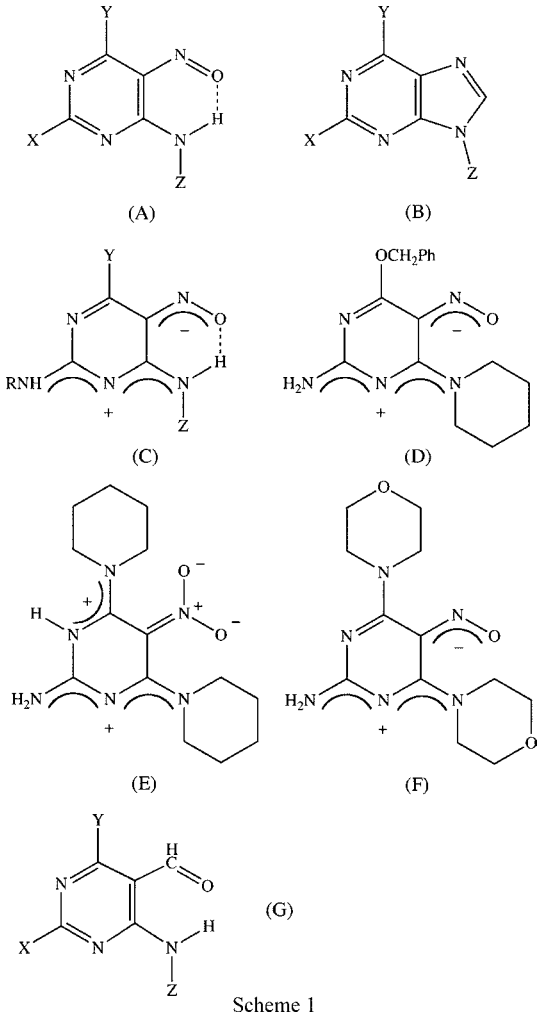


Scheme 1

While simply substituted pyrimidines generally exhibit effective planarity of the pyrimidine rings, we have found that where three contiguous substituents are present in the 4-, 5- and 6-positions, the rings are sometimes quite markedly non-planar, giving boat (Quesada *et al.*, 2004; Low *et al.*, 2007; Trilleras *et al.*, 2007), twist-boat (Melguizo *et al.*, 2003; Quesada *et al.*, 2003) or screw-boat (Low *et al.*, 2007) conformations, and comparison with less sterically congested analogues suggests that the steric clashes between neighbouring bulky substituents drive the ring distortion from planar to boat or twist-boat forms. However, it is striking that, even in compounds where the pyrimidine ring is distorted from planarity, the development of the polarized electronic structure does not seem to be significantly impaired by the distortion, as illustrated by examples such as (*D*) (Melguizo *et al.*, 2003), (*E*) (Quesada *et al.*, 2003) and (*F*) (Quesada *et al.*, 2004).

The combination of the observed biological activity of the nitrosopyrimidines and the fascinating interplay between their molecular structures and their strongly hydrogen-bonded crystal structures has led us to investigate the analogous 5-formyl systems (*G*), where the nitrosyl group (—N═O) is formally replaced by the isoelectronic formyl group (—CH═O). Here we report on the molecular and crystal structures of 12 such examples (Scheme 2), the conformations of which fall into two clear types: (I)–(V), (VII) and (X)–(XII), where the formyl O atom is oriented away from the chloro substituent, and (VI), (VIII) and (IX), where the formyl O atom is directed towards the chloro substituent.

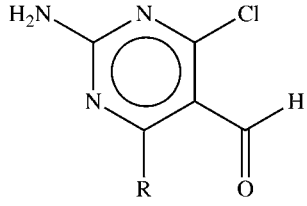

(I) R = NH(cyclohexyl)
(II) R = $NEt_2$
(III) R = N-morpholino
(IV) R = NMe(cyclohexyl)
(V) R = $NEt(CH_2Ph)$
(VII) R = $NH(CH_2Ph)$
(X) R = $NH(C_6H_4\text{-}NC_4H_4)$
(XI) R = $N(CH_2CH_2)_2NCH_2CH_2OH$
(XII) R = $N(CH_2)_5$

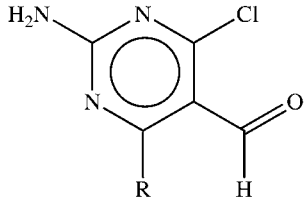

(VI) R = NEtPh
(VIII) R = NMePh
(IX) R = $NPh(CH_2Ph)$

Scheme 2

An early comparison (Low *et al.*, 1992) of the pair of corresponding C-nitroso and C-formyl uracil derivatives (XIII) and (XIV) (Scheme 3), which both crystallize from aqueous solution as stoichiometric monohydrates, found that these hydrates crystallize in different space groups [*Pnam* for (XIII) and *C*2/*c* for (XIV)]. However, these compounds adopt almost identical molecular conformations where the orientation of the formyl group in (XIV), and of the nitroso group in (XIII), mimic that found in (I)–(V), (VII) and (X)–(XII) (Scheme 2). Despite the close similarity in molecular structures, recent analysis (de la Torre *et al.*, 2007) of the crystal structures of (XIII) and (XIV) has shown that, although both compounds contain intramolecular N—H···O hydrogen bonds, the intermolecular hydrogen-bonding arrangements are entirely different. In (XIII) the molecular components are linked into sheets containing four different types of ring, while in (XIV) the components are linked into two interwoven three-dimensional frameworks; thus, overall a small change in molecular constitution leads to a large change in the supramolecular aggregation.

On the other hand, 5-formyluracil (XV) has recently been shown to adopt the alternative *syn* conformation with two adjacent and parallel carbonyl fragments (Portalone & Cola-

pietro, 2007). These authors also carried out a search of the Cambridge Structural Database (CSD; Allen, 2002) for structures containing 5-formyluracil or 5-formylthiouracil fragments: while only four structures were retrieved, all of these displayed the more common orientation of the formyl group.

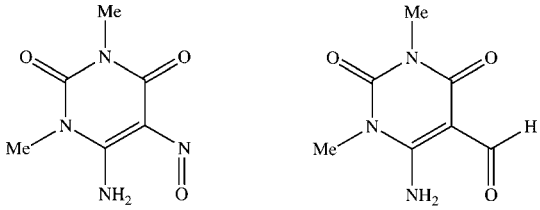

(XIII) (XIV)

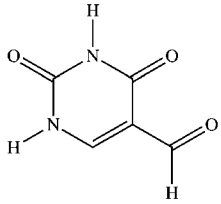

(XV)

Scheme 3

## 2. Experimental

### 2.1. Synthesis

Samples of (I)–(XII) were prepared by selective mono-substitution (Taylor & Gillespie, 1992; Quiroga *et al.*, 2008) of the 6-chloro substituent in 2-amino-4,6-dichloro-5-formylpyrimidine (Seela & Sterker, 1986). An equimolar mixture of the pyrimidine, the appropriate primary or secondary amine, and triethylamine as a base (1 mmol of each component) in ethanol (5 $cm^3$) was heated under reflux for 1 h in the case of primary amines and 3 h for secondary amines. The mixtures were cooled to ambient temperature and the resulting solid products were collected by filtration, washed with cold ethanol and dried in air [for (I), (VII) and (IX)] before being recrystallized from ethanol [for (II), (III), (VI), (VIII), (XI) and (XII)], methanol [for (V) and (X)] or dimethylformamide [for (IV)], to give yellow crystals suitable for single-crystal X-ray diffraction. 2-Amino-4-chloro-6-(cyclohexylamino)-5-formylpyrimidine (I), yield 60%, m.p. 407–408 K; $^1$H NMR: 1.15–1.41 (m, 5,), 1.45–1.55 (m, 1H), 1.60–1.72 (m, 2H), 1.80–1.90 (m, 2H), 3.90–4.05 (m, 1H), 7.59 (s, 1H, $NH_2$), 7.66 (s, 1H, $NH_2$), 9.14 (d, $J$ = 7.8 Hz, 1H,), 9.87 (s, 1H, CHO); $^{13}$C NMR: 24.1, 25.0, 32.0, 47.9, 100.7, 161.1, 162.4, 165.4, 187.4; MS $m/z$ (abundance %): 256 ($M$+2, 23), 254 ($M$, 55), 237 (27), 225 (22), 211 (32), 197 (74), 183 (27), 144 (100), 84 (18), 67 (37), 43 (85), 41 (86). HRMS calc. for $C_{11}H_{15}ClN_4O$: 254.0934, found: 254.0938. 2-Amino-4-chloro-6-(diethylamino)-5-formylpyrimidine (II), yield 70%, m.p. 404–405 K; $^1$H NMR: 1.11 (t, $J$ = 7.03 Hz, 6H), 3.42 (q, $J$ = 7.03 Hz, 4H), 7.35 (broad s, 1H, $NH_2$), 7.44 (broad s, 1H, $NH_2$), 9.86 (s, 1H, CHO); $^{13}$C NMR: 12.6, 44.0, 103.55, 160.9, 162.4, 165.6, 183.8 (CH═O); MS $m/z$ (abundance %): 230 ($M$+2, 28), 228 ($M$, 82), 213 (83), 211 (100), 199 (22), 195 (34), 183 (33), 181 (42), 171 (26), 157 (24), 129 (23), 93 (28), 84 (18), 67 (38), 44 (52), 43 (72), 42 (35). Anal.: calc. for $C_9H_{13}ClN_4O$: C 47.27, H 5.73, N 24.51; found: C 47.46, H 5.41, N 24.84. 2-Amino-4-chloro-5-formyl-6-morpholinopyrimidine (III), yield 81%, m.p. 449.2–450.2 K; $^1$H NMR: 3.46 (pt, $J$ = 4.4, 4.7 Hz, 4H, $CH_2$), 3.64 (pt, $J$ = 4.4, 4.7 Hz 4H, $CH_2$), 7.45–7.57 (broad s, 1H, $NH_2$), 7.60–7.70 (broad s, 1H, $NH_2$), 9.85 (s, 1H, CH═O); $^{13}$C NMR: 48.9, 66.1, 103.4, 161.2, 162.8, 166.6, 183.4 (CH═O); MS $m/z$ (abundance %): 244 ($M$+2, 4), 242 ($M$, 11), 225 (18), 129 (27), 94 (15), 69 (28), 55 (48), 43 (100). Anal.: calc. for $C_9H_{11}ClN_4O_2$: C 44.55, H 4.57, N 23.09; found: C 44.50, H 4.33, N 23.35. 2-Amino-4-chloro-6-(*N*-cyclohexyl-*N*-methylamino)-5-formylpyrimidine (IV), yield 80%, m.p. 468–469 K; $^1$H NMR: 1.07–1.17 (m, 1H), 1.22–1.35 (m, 2H), 1.45–1.57 (m, 2H), 1.57–1.65 (m, 1H), 1.66–1.72 (m, 2H), 1.72–1.80 (m-2H), 2.70 (s, 3H), 4.12–4.22 (m, 1H), 7.23–7.34 (broad s, 1H, $NH_2$), 7.45–7.34 (broad s, 1H, $NH_2$), 9.86 (s, 1H, CHO); $^{13}$C NMR: 25.0, 25.4, 29.2, 34.3, 57.8, 103.4, 160.7, 162.85, 165.6, 183.4 (CH═O); MS $m/z$ (abundance %): 270 ($M$+2, 13), 268 ($M$, 35), 251 (15), 239 (15), 225 (31), 213 (25), 211 (75), 197 (23), 185 (24), 183 (21), 158 (19), 129 (16), 81 (23), 67 (22), 55 (69), 43 (51), 42 (51), 41 (100). Anal.: calc. for $C_{12}H_{17}ClN_4O$: C 53.63, H 6.38, N 20.85; found: C 53.44, H 6.09, N 21.04. 2-Amino-6-(*N*-benzyl-*N*-ethylamino)-4-chloro-5-formylpyrimidine (V), yield 70%, m.p. 388.5 K; $^1$H NMR: 1.09 (t, $J$ = 7.0 Hz, 3H), 3.46 (q, $J$ = 7.0 Hz, 2H), 4.75 (s, 2H), 7.40–7.55 (m, 3H), 7.55–7.70 (m, 2H), 7.45 (broad s, 1H, $NH_2$), 7.57 (broad s, 1H, $NH_2$), 9.89 (s, 1H, CHO); $^{13}$C NMR: 12.5, 45.1, 51.2, 103.9, 127.0, 127.4, 128.3, 137.3, 161.0, 163.2, 165.7, 183.8 (CH═O); MS $m/z$ (abundance %): 292 ($M$+2, 5), 290 ($M$, 13), 261 (28), 199 (22), 191 (18), 91 (100), 77 (8), 65 (34), 43 (21). HRMS calcd. for $C_{14}H_{15}ClN_4O$: 290.0934; found: 290.0945. 2-Amino-4-chloro-6-(*N*-ethyl-*N*-phenylamino)-5-formylpyrimidine (VI), yield 96%, m.p. 445 K (decomp.); $^1$H NMR: 1.07 (t, $J$ = 7.0 Hz, 3H), 3.97 (q, $J$ = 7.0 Hz, 2H), 7.13 (t, $J$ = 7.4 Hz, 1H), 7.16 (d, $J$ = 7.5 Hz, 2H), 7.31 (t, $J$ = 7.4 Hz, 2H), 7.51 (broad s, 1H, $NH_2$), 7.57 (broad s, 1H, $NH_2$), 9.34 (s, 1H, CHO); $^{13}$C NMR: 12.5, 47.2, 104.2, 125.3, 125.6, 129.5, 145.7, 161.8, 162.4, 163.9, 183.2 (CH═O); MS $m/z$ (abundance %): 278 ($M$+2, 10), 276 ($M$, 34), 259 (35), 219 (21), 184 (14), 156 (14), 120 (24), 104 (14), 92 (15), 91 (15), 77 (100), 43 (47). Anal.: calcd. for $C_{13}H_{13}ClN_4O$: C 56.42, H 4.74, N 20.25; found: C 55.98, H 4.56, N 20.39. 2-Amino-6-(benzylamino)-4-chloro-5-formylpyrimidine (VII), yield 70%, m.p. 452–454 K; $^1$H NMR (p.p.m.): 4.68 (d, $J$ = 6.0 Hz, $CH_2$), 7.23 (m, 1H, CH), 7.33 (m, 4H, CH), 7.64 (broad s, 1H, $NH_2$), 7.72 (broad s, 1H, $NH_2$), 9.45 (t, $J$ = 6.0 Hz, 1H, NH), 9.92 (s, 1H, CH═O); $^{13}$C NMR (p.p.m.): 43.3, 101.0, 127.1, 127.4, 128.5, 138.6, 161.9, 162.4, 165.4, 187.5 (CH═O); MS $m/z$ (abundance %): 264 ($M$+2, 15), 262 ($M$, 40), 233 (28), 171 (12), 106 (44), 91 (100), 77 (18), 65 (52), 51 (14), 43 (35); HRMS MS $m/e$ calc. for $C_{12}H_{11}ClN_4O$ 262.0621; found 262.0612. Anal.: calc. for $C_{12}H_{11}ClN_4O$: C 54.87, H 4.22, N 21.33; found: C 54.69, H 3.79, N 21.60. 2-Amino-4-chloro-5-formyl-6-(*N*-methyl-*N*-phenylamino)pyrimidine (VIII), yield 94%, m.p. 453 K; $^1$H NMR: 3.39 (s, 3H), 7.13 (t, $J$ = 7.4 Hz, 1H), 7.18 (d, $J$ = 7.4 Hz, 2H), 7.31 (t, $J$ = 7.4 Hz, 2H), 7.56 (broad s, 1H, $NH_2$), 7.65 (broad s, 1H, $NH_2$), 9.43 (s, 1H, CHO); $^{13}$C NMR: 41.0,

**Table 1**
Experimental details.

| | (I) | (II) | (III) | (IV) | (V) |
|---|---|---|---|---|---|
| Crystal data | | | | | |
| Chemical formula | $C_{11}H_{15}ClN_4O$ | $C_9H_{13}ClN_4O$ | $C_9H_{11}ClN_4O_2$ | $C_{12}H_{17}ClN_4O$ | $C_{14}H_{15}ClN_4O$ |
| $M_r$ | 254.72 | 228.68 | 242.67 | 268.75 | 290.75 |
| Cell setting, space group | Triclinic, $P\overline{1}$ | Monoclinic, $P2_1/n$ | Monoclinic, $P2_1/c$ | Triclinic, $P\overline{1}$ | Triclinic, $P\overline{1}$ |
| Temperature (K) | 120 (2) | 120 (2) | 120 (2) | 120 (2) | 120 (2) |
| $a, b, c$ (Å) | 5.907 (2), 10.398 (3), 10.801 (2) | 11.328 (3), 8.0810 (4), 11.3849 (12) | 7.3540 (5), 8.2910 (13), 17.276 (3) | 8.5722 (6), 8.7195 (5), 8.7681 (7) | 7.9897 (5), 8.0922 (4), 11.2786 (7) |
| $\alpha, \beta, \gamma$ (°) | 110.86 (3), 94.19 (2), 96.00 (3) | 90.00, 98.709 (14), 90.00 | 90.00, 97.962 (9), 90.00 | 82.598 (6), 82.701 (5), 88.645 (5) | 91.602 (4), 107.220 (5), 91.776 (5) |
| $V$ (Å$^3$) | 612.2 (3) | 1030.2 (3) | 1043.2 (3) | 644.63 (8) | 695.66 (7) |
| $Z$ | 2 | 4 | 4 | 2 | 2 |
| $D_x$ (Mg m$^{-3}$) | 1.382 | 1.474 | 1.545 | 1.385 | 1.388 |
| Radiation type | Mo $K\alpha$ | Mo $K\alpha$ | Mo $K\alpha$ | Mo $K\alpha$ | Mo $K\alpha$ |
| $\mu$ (mm$^{-1}$) | 0.30 | 0.35 | 0.36 | 0.29 | 0.28 |
| Crystal form, colour | Plate, colourless | Plate, colourless | Block, colourless | Lath, colourless | Block, colourless |
| Crystal size (mm) | 0.48 × 0.28 × 0.08 | 0.37 × 0.36 × 0.08 | 0.43 × 0.27 × 0.25 | 0.55 × 0.29 × 0.12 | 0.29 × 0.28 × 0.21 |
| Data collection | | | | | |
| Diffractometer | Bruker–Nonius KappaCCD | Bruker–Nonius KappaCCD | Bruker–Nonius KappaCCD | Bruker–Nonius KappaCCD | Bruker–Nonius KappaCCD |
| Data collection method | $\varphi$ and $\omega$ scans | $\varphi$ and $\omega$ scans | $\varphi$ and $\omega$ scans | $\varphi$ and $\omega$ scans | $\varphi$ and $\omega$ scans |
| Absorption correction | Multi-scan | Multi-scan | Multi-scan | Multi-scan | Multi-scan |
| $T_{min}$ | 0.869 | 0.882 | 0.862 | 0.856 | 0.929 |
| $T_{max}$ | 0.976 | 0.973 | 0.916 | 0.966 | 0.944 |
| No. of measured, independent and observed reflections | 16 678, 2807, 2278 | 21 126, 2357, 1408 | 23 197, 2411, 1847 | 18 098, 2950, 2650 | 19 407, 3191, 2729 |
| Criterion for observed reflections | $I > 2\sigma(I)$ | $I > 2\sigma(I)$ | $I > 2\sigma(I)$ | $I > 2\sigma(I)$ | $I > 2\sigma(I)$ |
| $R_{int}$ | 0.045 | 0.099 | 0.057 | 0.018 | 0.026 |
| $\theta_{max}$ (°) | 27.5 | 27.5 | 27.5 | 27.5 | 27.5 |
| Refinement | | | | | |
| Refinement on | $F^2$ | $F^2$ | $F^2$ | $F^2$ | $F^2$ |
| $R[F^2 > 2\sigma(F^2)]$, $wR(F^2)$, $S$ | 0.039, 0.099, 1.08 | 0.058, 0.155, 1.08 | 0.038, 0.087, 1.08 | 0.031, 0.080, 1.08 | 0.034, 0.082, 1.12 |
| No. of reflections | 2807 | 2357 | 2411 | 2950 | 3191 |
| No. of parameters | 154 | 138 | 145 | 164 | 182 |
| H-atom treatment | Constrained to parent site | Constrained to parent site | Constrained to parent site | Constrained to parent site | Constrained to parent site |
| Weighting scheme | $w = 1/[\sigma^2(F_o^2) + (0.0393P)^2 + 0.3635P]$, where $P = (F_o^2 + 2F_c^2)/3$ | $w = 1/[\sigma^2(F_o^2) + (0.0594P)^2 + 1.3692P]$, where $P = (F_o^2 + 2F_c^2)/3$ | $w = 1/[\sigma^2(Fo2) + (0.0287P)^2 + 0.8135P]$, where $P = (F_o^2 + 2F_c^2)/3$ | $w = 1/[\sigma^2(F_o^2) + (0.0351P)^2 + 0.3109P]$, where $P = (F_o^2 + 2F_c^2)/3$ | $w = 1/[\sigma^2(F_o^2) + (0.0295P)^2 + 0.4094P]$, where $P = (F_o^2 + 2F_c^2)/3$ |
| $(\Delta/\sigma)_{max}$ | <0.0001 | <0.0001 | <0.0001 | <0.0001 | <0.0001 |
| $\Delta\rho_{max}$, $\Delta\rho_{min}$ (e Å$^{-3}$) | 0.25, −0.37 | 0.43, −0.36 | 0.26, −0.30 | 0.34, −0.24 | 0.28, −0.30 |

| | (VI) | (VII) | (VIII) | (IX) | (X) |
|---|---|---|---|---|---|
| Crystal data | | | | | |
| Chemical formula | $C_{13}H_{13}ClN_4O$ | $C_{12}H_{11}ClN_4O$ | $C_{12}H_{11}ClN_4O$ | $C_{18}H_{15}ClN_4O$ | $C_{15}H_{12}ClN_5O$ |
| $M_r$ | 276.72 | 262.70 | 262.70 | 338.79 | 313.75 |
| Cell setting, space group | Triclinic, $P\overline{1}$ | Triclinic, $P\overline{1}$ | Triclinic, $P\overline{1}$ | Triclinic, $P\overline{1}$ | Monoclinic, $P2_1/n$ |
| Temperature (K) | 120 (2) | 120 (2) | 120 (2) | 120 (2) | 120 (2) |
| $a, b, c$ (Å) | 8.1811 (12), 8.8325 (10), 9.3356 (6) | 7.0568 (7), 8.211 (2), 10.565 (3) | 6.9938 (6), 7.9544 (10), 10.7507 (14) | 6.5520 (11), 11.1012 (7), 11.4111 (4) | 7.5716 (7), 16.6432 (18), 10.9450 (7) |
| $\alpha, \beta, \gamma$ (°) | 81.844 (9), 82.015 (10), 73.041 (7) | 84.590 (16), 82.363 (14), 78.687 (14) | 81.191 (11), 82.469 (12), 87.333 (10) | 79.958 (5), 84.802 (9), 77.009 (9) | 90.00, 93.549 (6), 90.00 |
| $V$ (Å$^3$) | 635.38 (12) | 593.5 (2) | 585.71 (12) | 795.21 (15) | 1376.6 (2) |
| $Z$ | 2 | 2 | 2 | 2 | 4 |
| $D_x$ (Mg m$^{-3}$) | 1.446 | 1.470 | 1.490 | 1.415 | 1.514 |
| Radiation type | Mo $K\alpha$ | Mo $K\alpha$ | Mo $K\alpha$ | Mo $K\alpha$ | Mo $K\alpha$ |
| $\mu$ (mm$^{-1}$) | 0.30 | 0.32 | 0.32 | 0.25 | 0.29 |
| Crystal form, colour | Block, colourless | Block, colourless | Block, colourless | Plate, yellow | Lath, colourless |
| Crystal size (mm) | 0.56 × 0.46 × 0.24 | 0.41 × 0.20 × 0.13 | 0.37 × 0.27 × 0.18 | 0.58 × 0.48 × 0.05 | 0.51 × 0.25 × 0.10 |
| Data collection | | | | | |
| Diffractometer | Bruker–Nonius KappaCCD | Bruker–Nonius KappaCCD | Bruker–Nonius KappaCCD | Bruker–Nonius KappaCCD | Bruker–Nonius KappaCCD |

**Table 1 (continued)**

| | (VI) | (VII) | (VIII) | (IX) | (X) |
|---|---|---|---|---|---|
| Data collection method | $\varphi$ and $\omega$ scans | $\varphi$ and $\omega$ scans | $\varphi$ and $\omega$ scans | $\varphi$ and $\omega$ scans | $\varphi$ and $\omega$ scans |
| Absorption correction | Multi-scan | Multi-scan | Multi-scan | Multi-scan | Multi-scan |
| $T_{min}$ | 0.851 | 0.882 | 0.891 | 0.867 | 0.867 |
| $T_{max}$ | 0.932 | 0.960 | 0.945 | 0.988 | 0.972 |
| No. of measured, independent and observed reflections | 15 349, 2902, 2269 | 15 054, 2729, 1754 | 16 227, 2681, 2305 | 19 326, 3642, 2645 | 32 885, 3149, 2236 |
| Criterion for observed reflections | $I > 2\sigma(I)$ | $I > 2\sigma(I)$ | $I > 2\sigma(I)$ | $I > 2\sigma(I)$ | $I > 2\sigma(I)$ |
| $R_{int}$ | 0.035 | 0.061 | 0.030 | 0.038 | 0.057 |
| $\theta_{max}$ (°) | 27.5 | 27.5 | 27.5 | 27.5 | 27.5 |
| Refinement | | | | | |
| Refinement on | $F^2$ | $F^2$ | $F^2$ | $F^2$ | $F^2$ |
| $R[F^2 > 2\sigma(F^2)]$, $wR(F^2)$, $S$ | 0.040, 0.102, 1.11 | 0.052, 0.144, 1.06 | 0.033, 0.086, 1.09 | 0.040, 0.089, 1.09 | 0.045, 0.121, 1.11 |
| No. of reflections | 2902 | 2729 | 2681 | 3642 | 3149 |
| No. of parameters | 173 | 163 | 164 | 217 | 199 |
| H-atom treatment | Constrained to parent site | Constrained to parent site | Constrained to parent site | Constrained to parent site | Constrained to parent site |
| Weighting scheme | $w = 1/[\sigma^2(F_o^2) + (0.0368P)^2 + 0.5204P]$, where $P = (F_o^2 + 2F_c^2)/3$ | $w = 1/[\sigma^2(F_o^2) + (0.0602P)^2 + 0.5473P]$, where $P = (F_o^2 + 2F_c^2)/3$ | $w = 1/[\sigma^2(F_o^2) + (0.0397P)^2 + 0.2942P]$, where $P = (F_o^2 + 2F_c^2)/3$ | $w = 1/[\sigma^2(F_o^2) + (0.0241P)^2 + 0.4915P]$, where $P = (F_o^2 + 2F_c^2)/3$ | $w = 1/[\sigma^2(F_o^2) + (0.0507P)^2 + 1.2389P]$, where $P = (F_o^2 + 2F_c^2)/3$ |
| $(\Delta/\sigma)_{max}$ | <0.0001 | <0.0001 | 0.001 | <0.0001 | <0.0001 |
| $\Delta\rho_{max}$, $\Delta\rho_{min}$ (e Å$^{-3}$) | 0.31, −0.36 | 0.50, −0.59 | 0.28, −0.28 | 0.26, −0.28 | 0.36, −0.48 |

| | (XI) | (XII) |
|---|---|---|
| Crystal data | | |
| Chemical formula | $C_{11}H_{16}ClN_5O_2$ | $C_{10}H_{13}ClN_4O$ |
| $M_r$ | 285.74 | 240.69 |
| Cell setting, space group | Triclinic, $P\bar{1}$ | Monoclinic, $Cc$ |
| Temperature (K) | 120 (2) | 120 (2) |
| $a$, $b$, $c$ (Å) | 7.2147 (6), 8.8563 (10), 10.2855 (12) | 14.4681 (17), 11.1378 (17), 7.4534 (7) |
| $\alpha$, $\beta$, $\gamma$ (°) | 84.856 (10), 85.296 (10), 79.092 (7) | 90.00, 116.535 (7), 90.00 |
| $V$ (Å$^3$) | 641.28 (12) | 1074.5 (2) |
| $Z$ | 2 | 4 |
| $D_x$ (Mg m$^{-3}$) | 1.480 | 1.488 |
| Radiation type | Mo $K\alpha$ | Mo $K\alpha$ |
| $\mu$ (mm$^{-1}$) | 0.31 | 0.34 |
| Crystal form, colour | Block, colourless | Block, colourless |
| Crystal size (mm) | 0.58 × 0.29 × 0.22 | 0.30 × 0.26 × 0.15 |
| Data collection | | |
| Diffractometer | Bruker–Nonius KappaCCD | Bruker–Nonius KappaCCD |
| Data collection method | $\varphi$ and $\omega$ scans | $\varphi$ and $\omega$ scans |
| Absorption correction | Multi-scan | Multi-scan |
| $T_{min}$ | 0.843 | 0.896 |
| $T_{max}$ | 0.936 | 0.951 |
| No. of measured, independent and observed reflections | 15 336, 2936, 2402 | 12 891, 2460, 1972 |
| Criterion for observed reflections | $I > 2\sigma(I)$ | $I > 2\sigma(I)$ |
| $R_{int}$ | 0.024 | 0.050 |
| $\theta_{max}$ (°) | 27.5 | 27.5 |
| Refinement | | |
| Refinement on | $F^2$ | $F^2$ |
| $R[F^2 > 2\sigma(F^2)]$, $wR(F^2)$, $S$ | 0.038, 0.102, 1.13 | 0.038, 0.087, 1.11 |
| No. of reflections | 2936 | 2460 |
| No. of parameters | 173 | 145 |
| H-atom treatment | Constrained to parent site | Constrained to parent site |
| Weighting scheme | $w = 1/[\sigma^2(F_o^2) + (0.0442P)^2 + 0.4199P]$, where $P = (F_o^2 + 2F_c^2)/3$ | $w = 1/[\sigma^2(F_o^2) + (0.0345P)^2 + 0.8328P]$, where $P = (F_o^2 + 2F_c^2)/3$ |
| $(\Delta/\sigma)_{max}$ | 0.001 | <0.0001 |
| $\Delta\rho_{max}$, $\Delta\rho_{min}$ (e Å$^{-3}$) | 0.31, −0.27 | 0.33, −0.28 |
| Absolute structure | – | Flack (1983), 1219 Friedel pairs |
| Flack parameter | – | 0.07 (7) |

104.4, 124.5, 125.5, 129.4, 147.7, 161.7, 162.7, 164.4, 183.2 (CH═O); MS *m*/*z* (abundance %): 264 (*M*+2, 34), 262 (*M*, 100), 245 (94), 233 (45), 219 (10), 210 (21), 198 (40), 184 (26), 156 (20), 129 (24), 106 (41), 86 (13), 77 (87), 51 (48), 43 (25). Anal.: calc. for $C_{12}H_{11}ClN_4O$: C 54.86, H 4.22, N 21.33; found: C 55.42, H 4.24, N 21.51. 2-Amino-6-(*N*-benzyl-*N*-phenylamino)-4-chloro-5-formylpyrimidine (IX), yield 70%, m.p. 439–441 K; $^1$H NMR: 5.28 (s, 2H, $CH_2$), 7.06–7.33 (m, 10H, CH), 7.56 (broad s, 1H, $NH_2$), 7.66 (broad s, 1H, $NH_2$), 9.44 (s, 1H, CH═O); $^{13}$C NMR: 54.6, 104.5, 124.3, 125.3, 126.9, 127.7, 128.1, 129.3, 137.6, 146.2, 161.7, 162.7, 164.1, 183.3 (CH═O); MS *m*/*z* (abundance %): 340 (*M*+2, 8), 338 (*M*, 23), 309 (14), 247 (6), 91 (100), 77 (20), 65 (26). HRMS calc. for $C_{18}H_{15}ClN_4O$ 338.0934; found 338.0940. 2-Amino-4-chloro-5-formyl-6-(2-(1*H*-pyrrol-1-yl)phenylamino)pyrimidine (X), yield 60%, m.p. 475–476 K; $^1$H NMR: 6.19 (t, $J$ = 2.3 Hz, 2H, CH), 6.87 (t, $J$ = 2.3 Hz, 2H, CH), 7.27–7.34 (m, 2H, CH), 7.37–7.42 (m, 1H, CH), 7.77 (broad s, 1H, $NH_2$), 7.85 (broad s, 1H, $NH_2$), 8.09–8.12 (dd, $J$ = 1.2 Hz, 8.0 Hz, 1H, CH), 9.85 (s, 1H, CH═O), 10.72 (s, 1H); $^{13}$C NMR: 101.4, 109.5, 121.6, 125.8, 126.2, 126.7, 127.5, 132.4, 134.2, 160.7, 162.2, 165.3, 187.5 (CH═O); MS *m*/*z* (abundance %): 315 (*M*+2), 313 (*M*, 100), 284 (43), 246 (38), 207 (33), 157 (34), 68 (21), 43 (20); HRMS calc. for $C_{15}H_{12}ClN_5O$: 313.0730, found: 313.0732. Anal.: calc. for $C_{15}H_{12}ClN_5O{\cdot}0.5H_2O$: C 55.82, H 4.37, N 21.70; found: C 55.42, H 4.24, N 21.51. 2-Amino-4-chloro-5-formyl-6-(4-(2-hydroxyethyl)piperazin-1-yl)pyrimidine (XI), yield 72%, m.p. 449 K; $^1$H NMR: 2.39 (t, $J$ = 6.2 Hz, 2H, $CH_2$), 2.46 (m, 4H, $CH_2$), 3.45 (m, 4H, $CH_2$), 3.50 (q, $J$ = 6.0 Hz, 2H, $CH_2$), 4.40 (t, $J$ = 5.4 Hz, 1H, OH), 7.47 (broad s, 1H, $NH_2$), 7.58 (broad s, 1H, $NH_2$), 9.83 (s, 1H, CH═O); $^{13}$C NMR: 48.3, 53.1, 58.4, 60.2, 103.3, 161.2, 162.6, 166.5, 183.3 (CH═O); MS *m*/*z* (abundance %): 287 (*M*+2, 7), 285 (*M*, 18), 254 (17), 195 (12), 183 (11), 169 (10), 100 (97), 88 (25), 70 (26), 56 (57), 43 (37), 42 (100); HRMS calc. for $C_{11}H_{16}ClN_5O_2$ 285.0993, found 285.1002. 2-Amino-4-chloro-5-formyl-6-(piperidin-1-yl)pyrimidine (XII), yield 71%, m.p. 446–447 K; $^1$H NMR: 1.57 (m, 6H, $CH_2$), 3.42 (m, 4H, $CH_2$), 7.38 (broad s, 1H, $NH_2$), 7.52 (broad s, 1H, $NH_2$), 9.83 (s, 1H, CH═O); $^{13}$C NMR: 23.4, 25.6, 49.4, 103.3, 161.2, 162.6, 166.3, 1873.3 (CH═O); MS *m*/*z* (abundance %): 240 (*M*, 35), 223 (100), 188 (15), 84 (21), 41 (23). HRMS calc. for $C_{10}H_{13}ClN_4O$: 240.0778; found: 240.0777.

### 2.2. Data collection, structure solution and refinement

Details of cell data, data collection and structure solution and refinement are summarized in Table 1 (Burla *et al.*, 2005; Duisenberg *et al.*, 2000, 2003; Ferguson, 1999; Hooft, 1999; McArdle, 2003; Otwinowski & Minor, 1997; Sheldrick, 2003, 2008; Spek, 2003). Unique assignments of space groups were made from the systematic absences for each of compounds (II), (III) and (X). For (XII) the systematic absences permitted *C*2/*c* and *Cc* as possible space groups: *Cc* was selected and subsequently confirmed by structure analysis. The correct orientation of the structure with respect to the polar axis directions was established by means of the Flack parameter (Flack, 1983), 0.07 (7) with 1219 Friedel pairs. Crystals of (I), (IV)–(IX) and (XI) are all triclinic and for each the space group $P\bar{1}$ was selected and subsequently confirmed by structure analysis. The structures were all solved by direct methods using *SHELXS*97 (Sheldrick, 2008) and refined on $F^2$ with all data using *SHELXL*97 (Sheldrick, 2008). A weighting scheme based upon $P = [F_o^2 + 2F_c^2]/3$ was employed in order to reduce statistical bias (Wilson, 1976). All H atoms were located in difference maps and then treated as riding atoms with distances C—H 0.95 (aromatic, formyl and heterocyclic), 0.98 ($CH_3$), 0.99 ($CH_2$) or 1.00 Å (aliphatic CH), N—H 0.86–1.03 Å and O—H 0.84 Å, and with $U_{iso}$(H) = $kU_{eq}$(carrier), where $k$ = 1.5 for the methyl groups, and $k$ = 1.2 for all other H atoms. Supramolecular analyses were made, and the diagrams were prepared with the aid of *PLATON* (Spek, 2003). Fig. 1 shows the independent components and conformations of (I)–(XII) with the atom-labelling schemes, and Figs. 2–10 show aspects of the supramolecular structures. Selected geometric parameters are given in Table 2 and details of the hydrogen bonding are in Table 3.[1]

## 3. Results and discussion

### 3.1. Molecular dimensions and conformations

**3.1.1. Shape of the pyrimidine rings**. In (I) and (VII)–(X) the pyrimidine rings do not deviate significantly from planarity, and this is as expected for unperturbed rings of this type. However, for the remaining compounds studied here, the pyrimidine rings are all markedly non-planar, as the ring-puckering parameters (Cremer & Pople, 1975) clearly show [Table 2, section (i)]. The pyrimidine ring conformation in (VI) approximates to a boat form, for which the idealized puckering angles are $\theta$ = 90° and $\varphi$ = (60$n$)°, where $n$ represents an integer. The conformation in each of compounds (III)–(V) is close to the twist-boat form, for which the idealized puckering angles are $\theta$ = 90° and $\varphi$ = (60$n$ + 30)°, while conformations intermediate between boat and twist-boat are found in (II) and (XI), and a conformation between twist-boat and screw-boat is found in (XII). In all cases the degree to which the pyrimidine rings are distorted from planarity is perhaps best illustrated by the deviations of the immediate ring-substituent atoms from the mean planes of the pyrimidine ring atoms [Table 2, section (ii)].

For (II)–(VI), (XI) and (XII), having puckered pyrimidine rings, the displacements of the substituent atoms are such that atoms N1 and C51 are always displaced to the opposite side of the ring from atoms Cl4 and N61, consistent with the sense of the ring puckering itself. For this subset of compounds, where the displacement of atom C51 reaches a maximum value of 0.756 (2) Å in (III), it is tempting to associate the ring puckering with the steric congestion arising from the substituents at ring atoms C4, C5 and C6. By contrast, in (I) and (VII)–(X) where the pyrimidine rings are effectively planar, the substi-

[1] Supplementary data for this paper are available from the IUCr electronic archives (Reference: BM5057). Services for accessing these data are described at the back of the journal.

**Table 2**
Selected geometric parameters (Å,°).

| | *Q* | *θ*† | *φ*† |
|---|---|---|---|
| (i) Pyrimidine ring-puckering parameters | | | |
| (I)‡ | | | |
| (II) | 0.174 (3) | 95.2 (10) | 77 (11) |
| (III) | 0.1964 (17) | 81.6 (5) | 260.8 (5) |
| (IV) | 0.1956 (12) | 82.6 (4) | 262.3 (8) |
| (V) | 0.1529 (14) | 84.7 (5) | 157.9 (5) |
| (VI) | 0.0923 (18) | 99.0 (11) | 66.3 (11) |
| (VII)‡ | | | |
| (VIII)‡ | | | |
| (IX)‡ | | | |
| (X)‡ | | | |
| (XI) | 0.1457 (16) | 93.5 (6) | 78.6 (6) |
| (XII) | 0.174 (3) | 79.1 (10) | 262.3 (9) |

| | N2 | Cl4 | C51 | O51 | N61 |
|---|---|---|---|---|---|
| (ii) Substituent displacements§ (Å) from mean plane of pyrimidine ring | | | | | |
| (I) | +0.023 (2) | −0.058(2) | +0.029 (2) | 0.000 (2) | +0.010 (2) |
| (II) | +0.307 (2) | −0.159 (2) | +0.622 (3) | +1.199 (2) | −0.340 (2) |
| (III) | +0.330 (2) | −0.127 (2) | +0.756 (2) | +1.243 (2) | −0.378 (2) |
| (IV) | +0.326 (2) | −0.136 (2) | +0.707 (2) | +1.241 (2) | −0.442 (2) |
| (V) | +0.272 (2) | −0.052 (2) | +0.631 (2) | +1.244 (2) | −0.299 (2) |
| (VI) | +0.154 (2) | −0.147 (2) | +0.484 (2) | +0.618 (2) | −0.120 (2) |
| (VII) | +0.028 (2) | −0.004 (2) | +0.014 (3) | +0.014 (2) | +0.023 (2) |
| (VIII) | +0.012 (2) | +0.133 (2) | +0.280 (2) | +0.027 (2) | −0.077 (2) |
| (IX) | −0.066 (2) | +0.029 (2) | +0.304 (2) | +0.033 (2) | −0.121 (2) |
| (X) | +0.085 (2) | +0.018 (2) | +0.058 (2) | +0.092 (2) | −0.090 (2) |
| (XI) | +0.261 (2) | −0.058 (2) | +0.633 (2) | +0.988 (2) | −0.232 (2) |
| (XII) | +0.276 (2) | −0.121 (2) | +0.741 (3) | +1.274 (2) | −0.359 (2) |

| | N1—C2 | C2—N3 | N3—C4 | C4—C5 | C5—C6 | C6—N1 |
|---|---|---|---|---|---|---|
| (iii) Pyrimidine ring distances | | | | | | |
| (I) | 1.336 (2) | 1.366 (2) | 1.311 (2) | 1.392 (2) | 1.439 (2) | 1.346 (2) |
| (II) | 1.326 (4) | 1.367 (4) | 1.308 (4) | 1.398 (4) | 1.440 (4) | 1.349 (4) |
| (III) | 1.326 (2) | 1.376 (2) | 1.308 (2) | 1.399 (3) | 1.449 (2) | 1.344 (2) |
| (IV) | 1.3301 (15) | 1.3775 (15) | 1.3082 (16) | 1.4023 (16) | 1.4487 (15) | 1.3441 (15) |
| (V) | 1.3292 (17) | 1.3687 (17) | 1.3105 (18) | 1.3994 (19) | 1.4436 (18) | 1.3464 (17) |
| (VI) | 1.338 (2) | 1.366 (2) | 1.318 (2) | 1.395 (2) | 1.438 (2) | 1.337 (2) |
| (VII) | 1.338 (3) | 1.370 (3) | 1.312 (3) | 1.399 (4) | 1.440 (4) | 1.351 (3) |
| (VIII) | 1.3439 (17) | 1.3574 (17) | 1.3249 (18) | 1.3888 (19) | 1.4290 (19) | 1.3330 (18) |
| (IX) | 1.342 (2) | 1.355 (2) | 1.323 (2) | 1.390 (2) | 1.432 (2) | 1.339 (2) |
| (X) | 1.343 (3) | 1.370 (3) | 1.312 (3) | 1.399 (3) | 1.438 (3) | 1.326 (3) |
| (XI) | 1.338 (2) | 1.379 (2) | 1.300 (2) | 1.404 (2) | 1.453 (2) | 1.334 (2) |
| (XII) | 1.338 (3) | 1.367 (3) | 1.300 (3) | 1.405 (3) | 1.438 (3) | 1.345 (3) |

| | C2—N2 | C5—C51 | C51—O51 | C6—N61 | C4—C5—C51—O51 |
|---|---|---|---|---|---|
| (iv) Exocyclic distances and torsional angles | | | | | |
| (I) | 1.338 (2) | 1.446 (2) | 1.229 (2) | 1.335 (2) | −177.51 (17) |
| (II) | 1.325 (4) | 1.450 (4) | 1.219 (4) | 1.348 (4) | −153.8 (3) |
| (III) | 1.333 (2) | 1.441 (2) | 1.229 (2) | 1.338 (2) | 160.36 (18) |
| (IV) | 1.3340 (15) | 1.4441 (17) | 1.2290 (15) | 1.3405 (15) | 156.72 (15) |
| (V) | 1.3394 (18) | 1.4549 (19) | 1.2230 (17) | 1.3469 (17) | 150.42 (14) |
| (VI) | 1.334 (2) | 1.467 (2) | 1.211 (2) | 1.365 (2) | 12.0 (2) |
| (VII) | 1.332 (3) | 1.437 (4) | 1.227 (3) | 1.338 (3) | 180.0 (3) |
| (VIII) | 1.3354 (17) | 1.4739 (19) | 1.2085 (18) | 1.3663 (17) | −30.8 (2) |
| (IX) | 1.338 (2) | 1.476 (2) | 1.208 (2) | 1.367 (2) | 34.1 (3) |
| (X) | 1.328 (3) | 1.438 (3) | 1.233 (3) | 1.355 (3) | 179.0 (2) |
| (XI) | 1.325 (2) | 1.441 (2) | 1.230 (2) | 1.348 (2) | −167.22 (16) |
| (XII) | 1.337 (3) | 1.439 (4) | 1.233 (3) | 1.344 (3) | 157.1 (3) |

† The puckering angles are calculated for the atom sequences (N1, C2, N3, C4, C5, C6). ‡ In (I) and (VII)–(X) the pyrimidine rings are effectively planar. § Signs + and − indicate displacements to opposite sides of the mean plane, with the sign of the N2 displacement always chosen to be positive.

tuent displacements are always much smaller with no consistent pattern in the direction of the displacements of atoms Cl4, C51 and N61.

**3.1.2. Orientation of the formyl group**. A number of factors can be considered as plausible contributors to the orientation of the formyl group, where the orientation in (VI), (VIII) and (IX) differs from that in all the other compounds studied here.

(i) Intramolecular N—H···O hydrogen bonds. The occurrence of an intramolecular hydrogen bond is possible only in (I), (VII) and (X), as these are the only compounds with an appropriately available N—H: in all three, this hydrogen bond is formed (Table 3). However, the inability of the other compounds to form this bond indicates that it cannot be the decisive factor.

(ii) Intramolecular C—H···$\pi$(arene) hydrogen bonds. In each of compounds (VI), (VIII) and (IX) there is an aryl ring in approximately the correct position to form an intramolecular C—H···$\pi$(arene) hydrogen bond, but in every case the formyl H atom is, in fact, too remote from the aryl ring for any significant interaction to occur.

(iii) Electrostatic factors. It may be expected that the C4—Cl4 bond is polarized with the Cl carrying a partial negative charge: since the formyl O atom also carries such a charge, then the mutual repulsion of such charges might be expected to make the conformation found in (VI), (VIII) and (IX) the unfavourable one, in the absence of any other factors.

(iv) Intermolecular hydrogen bonds. In all compounds except (I), (VIII), (IX) and (XI), the formyl O atom acts as the acceptor in an intermolecular N—H···O hydrogen bond, while in (IX) and (XI), respectively, it acts as the acceptor in C—H···O and O—H···O hydrogen bonds. In (I) the only participation of this O atom is in an intramolecular hydrogen bond, and in (VIII) it is not involved in any hydrogen bond. While the formation of intermolecular hydrogen bonds appears to be a fairly general phenomenon, it certainly cannot be invoked to interpret the anomalous conformation in (VIII).

**3.1.3. Molecular dimensions**. The bond distances within the pyrimidine rings and those involving the immediate ring substituents (Table 2) show a number of systematic features which reflect the likely molecular-electronic structures. Firstly, amongst the C—N bonds, the ring bond N3—C4 is consistently the shortest bond of this type, while the distances for the ring

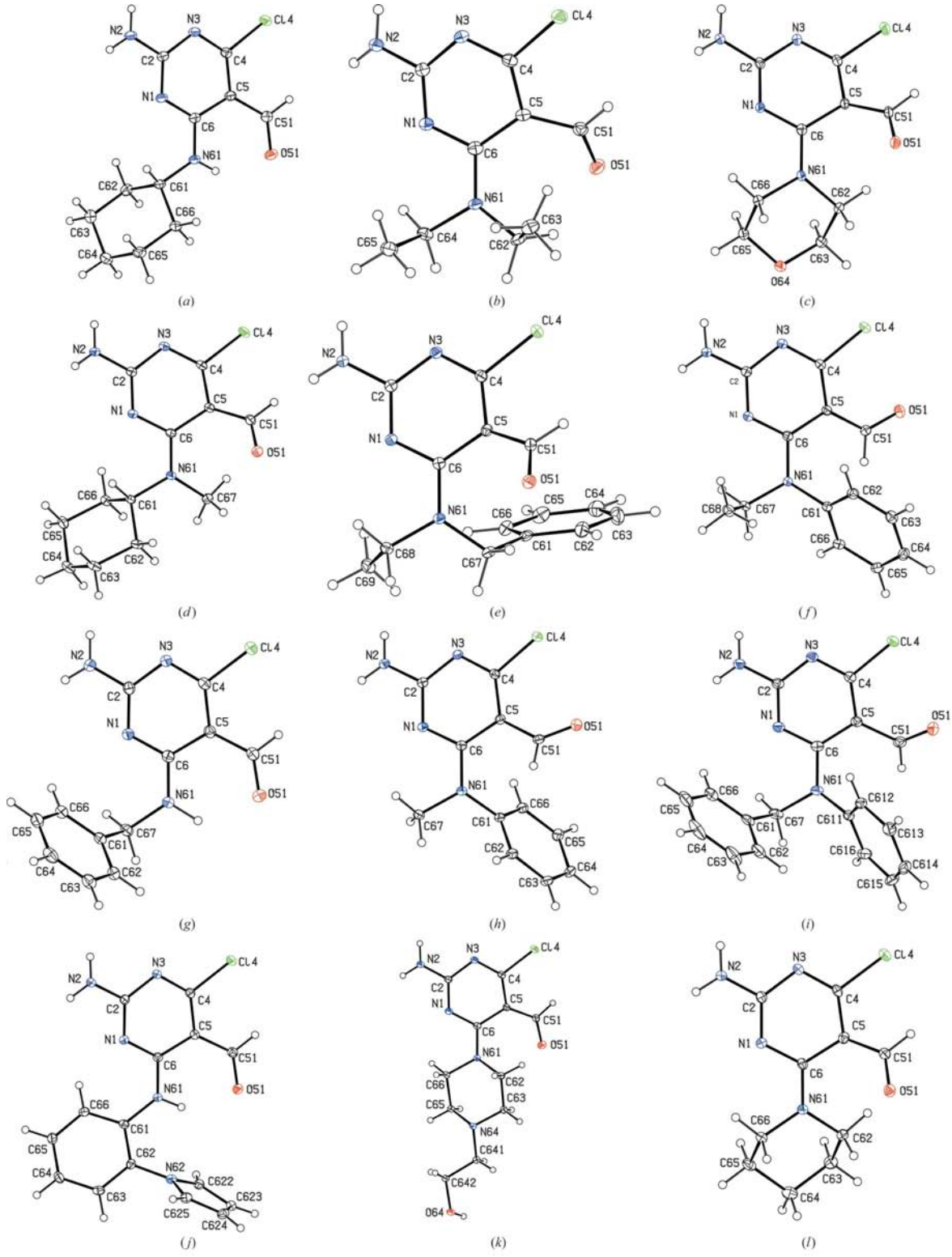


**Figure 1**
The molecular structures of (I)–(XII) showing the atom-labelling schemes: (*a*) (I); (*b*) (II); (*c*) (III); (*d*) (IV); (*e*) (V); (*f*) (VI); (*g*) (VII); (*h*) (VIII); (*i*) (IX); (*j*) (X); (*k*) (XI); (*l*) (XII). Displacement ellipsoids are drawn throughout at the 30% probability level.

**Table 3**
Parameters (Å, °) for hydrogen bonds and short intramolecular contacts.

| $D$—H···$A$ | $D$—H | H···$A$ | $D$···$A$ | $D$—H···$A$ | Motif |
|---|---|---|---|---|---|
| (I) | | | | | |
| N2—H2$B$···N3$^{i}$ | 0.86 | 2.11 | 2.966 (2) | 179 | $R_2^2(8)$ |
| N61—H61···O51 | 0.86 | 2.02 | 2.725 (2) | 139 | $S(6)$ |
| (II) | | | | | |
| N2—H2$A$···O51$^{ii}$ | 0.86 | 2.16 | 2.986 (3) | 160 | $R_2^2(16)$ |
| N2—H2$B$···N3$^{iii}$ | 0.86 | 2.17 | 3.027 (3) | 176 | $R_2^2(8)$ |
| (III) | | | | | |
| N2—H2$A$···O51$^{ii}$ | 0.86 | 2.11 | 2.955 (2) | 169 | $R_2^2(16)$ |
| N2—H2$B$···N3$^{iii}$ | 0.86 | 2.17 | 3.023 (2) | 171 | $R_2^2(8)$ |
| (IV) | | | | | |
| N2—H2$A$···O51$^{iv}$ | 0.86 | 2.14 | 2.9672 (14) | 160 | $R_2^2(16)$ |
| N2—H2$B$···N3$^{v}$ | 0.86 | 2.21 | 3.0727 (14) | 178 | $R_2^2(8)$ |
| (V) | | | | | |
| N2—H2$A$···O51$^{iv}$ | 0.86 | 2.18 | 3.0148 (16) | 164 | $R_2^2(16)$ |
| N2—H2$B$···N3$^{vi}$ | 0.86 | 2.19 | 3.0407 (17) | 172 | $R_2^2(8)$ |
| C65—H65···Cg1$^{ii}$† | 0.95 | 2.86 | 3.7061 (17) | 149 | – |
| C68—H68$A$···Cg1$^{iv}$† | 0.99 | 2.66 | 3.4643 (15) | 138 | – |
| (VI) | | | | | |
| N2—H2$A$···O51$^{vii}$ | 0.88 | 2.23 | 3.031 (2) | 152 | $C(8)$‡ |
| N2—H2$B$···N3$^{iii}$ | 0.88 | 2.32 | 3.178 (2) | 162 | $R_2^2(8)$‡ |
| (VII) | | | | | |
| N2—H2$B$···N3$^{viii}$ | 0.88 | 2.14 | 3.020 (3) | 176 | $R_2^2(8)$ |
| N61—H61···O51 | 1.03 | 1.97 | 2.727 (3) | 128 | $S(6)$ |
| N61—H61···O51$^{vi}$ | 1.03 | 2.10 | 2.953 (3) | 138 | $R_2^2(4)$ |
| (VIII) | | | | | |
| N2—H2$A$···Cg2$^{iii}$† | 0.86 | 2.74 | 3.5257 (14) | 152 | – |
| N2—H2$B$···N3$^{ix}$ | 0.86 | 2.18 | 3.0374 (17) | 178 | $R_2^2(8)$ |
| (IX) | | | | | |
| N2—H2$B$···N3$^{ix}$ | 0.88 | 2.10 | 2.981 (2) | 178 | $R_2^2(8)$ |
| C614—H614···O51$^{vi}$ | 0.95 | 2.48 | 3.352 (3) | 153 | $R_2^2(20)$ |
| (X) | | | | | |
| N2—H2$A$···O51$^{x}$ | 0.88 | 2.22 | 3.038 (2) | 158 | $C(8)$§ |
| N2—H2$B$···N3$^{ii}$ | 0.88 | 2.17 | 3.032 (3) | 178 | $R_2^2(8)$§ |
| N61—H61···O51 | 0.86 | 1.98 | 2.707 (2) | 141 | $S(6)$ |
| (XI) | | | | | |
| N2—H2$A$···O64$^{ii}$ | 0.88 | 2.03 | 2.909 (2) | 174 | $R_2^2(24)$ |
| N2—H2$B$···N3$^{xi}$ | 0.88 | 2.17 | 3.053 (3) | 177 | $R_2^2(8)$ |
| O64—H64···O51$^{iv}$ | 0.84 | 1.99 | 2.824 (2) | 173 | $R_2^2(24)$ |
| (XII) | | | | | |
| N2—H2$A$···O51$^{xii}$ | 0.88 | 2.04 | 2.902 (3) | 166 | $C(8)$¶ |
| N2—H2B···N1$^{xiii}$ | 0.88 | 2.32 | 3.144 (3) | 155 | $C(4)$¶ |

Symmetry codes: (i) $2-x, 2-y, 1-z$; (ii) $1-x, 1-y, 1-z$; (iii) $1-x, -y, 1-z$; (iv) $1-x, 1-y, -z$; (v) $1-x, 2-y, -z$; (vi) $-x, 1-y, -z$; (vii) $-1+x, y, z$; (viii) $2-x, -y, -z$; (ix) $2-x, 1-y, 1-z$; (x) $\frac{1}{2}+x, \frac{1}{2}-y, \frac{1}{2}+z$; (xi) $3-x, -y, 1-z$; (xii) $-\frac{1}{2}+x, \frac{1}{2}-y, -\frac{1}{2}+z$; (xiii) $x, 1-y, \frac{1}{2}+z$. † Cg1 and Cg2 are the centroids of the rings (N1, C2, N3, C4, C5, C6) and (C61–C66), respectively. ‡ Two intermolecular hydrogen bonds in combination generate a chain of alternating $R_2^2(8)$ and $R_4^4(16)$ rings. § Two intermolecular hydrogen bonds in combination generate a sheet of $R_2^2(8)$ and $R_6^6(32)$ rings. ¶ Two intermolecular hydrogen bonds in combination generate a three-dimensional framework structure.

bonds N1—C2 and N1—C6, and the exocyclic bond C2—N2 are always very similar. The exocyclic bond C6—N61 is similar in length to the bonds N1—C2, N1—C6 and C2—N2 in (I)–(V), (VII) and (XII), but it is significantly longer than these bonds in (VI) and (VIII)–(XI): the longest values for C6—N61 occur in (VI), (VIII) and (IX), which are just those examples where the orientation of the formyl O atom is towards rather than away from the chloro substituent. The double-bond contribution to the C2—N2 bond deduced from the solid-state dimensions is also apparent in the $^1$H NMR spectra in solution, where the 2-amino resonance appears as two singlets, usually broad, as a result of restricted rotation.

Of the two ring C—C bonds, while the C5—C6 bond is consistently longer than C4—C5, the maximum difference between these bond lengths is only 0.050 (2) Å, in (III), and this is small compared with a difference of *ca* 0.160 Å expected between the lengths of single and double bonds formed between two planar C atoms (Allen *et al.*, 1987). Finally, the aldehyde C—O bond is always long for its type [mean value (Allen *et al.*, 1987) 1.192 Å], while the C5—C51 bond is always short for its type (mean value 1.488 Å).

These observations, taken all together indicate that the polarized forms [*H*, see Scheme 4, and *J* for (VI), (VIII) and (IX)] are significant contributors to the overall molecular electronic structures in addition to the delocalized hetero-aromatic form (*K*), but that classically localized forms such as (*L*) are not major contributors.

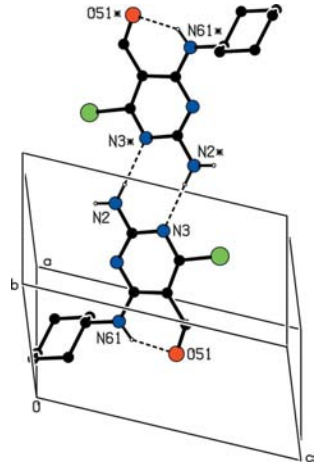


**Figure 2**
Part of the crystal structure of (I) showing the formation of a centrosymmetric hydrogen-bonded $R_2^2(8)$ dimer. For the sake of clarity the H atoms bonded to C atoms have been omitted. The atoms marked with an asterisk (*) are at the symmetry position $(2-x, 2-y, 1-z)$.

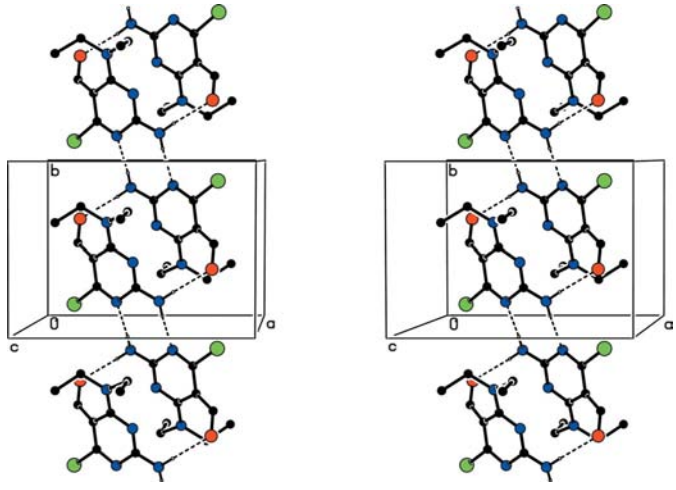


**Figure 3**
A stereoview of part of the crystal structure of (II) showing the formation of a chain of edge-fused hydrogen-bonded $R_2^2(8)$ and $R_2^2(16)$ rings along [010]. For the sake of clarity the H atoms bonded to C atoms have been omitted.

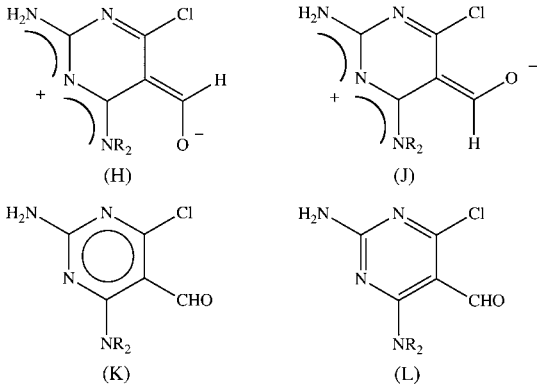


Scheme 4

It is noteworthy that as found in several previous examples (Melguizo *et al.*, 2003; Quesada *et al.*, 2003, 2004; Low *et al.*, 2007; Trilleras *et al.*, 2007), the distortion from planarity of the pyrimidine rings does not seem to impair the development of polarized electronic structures. The overlap and resonance integrals involving neighbouring atoms, at their optimum in rings which are planar, are evidently diminished only modestly by ring puckering of the magnitude observed here.

### 3.2. Supramolecular structures

The supramolecular aggregation is dominated by hydrogen bonds of the types N—H···N and N—H···O, augmented by hydrogen bonds of O—H···O, N—H···$\pi$ and C—H···$\pi$ types in (XI), (VIII) and (V), respectively (Table 3). Of the short intermolecular contacts indicated by *PLATON* (Spek, 2003) as possible hydrogen bonds we have rejected all of those involving methyl C—H bonds as the potential donors. Not only are methyl C—H bonds expected to be of rather low acidity but, in general, methyl groups $CH_3$-*E* (where *E* represents the atom to which the methyl group is bonded) undergo extremely fast rotation about the C—*E* bonds even in the solid state, as shown by solid-state NMR spectroscopy (Riddell & Rogerson, 1996, 1997). Such contacts of C—H···$\pi$ type occur in (V), while similar contacts of C—H···N type occur in (VIII). In each case, however, the fast rotation of the methyl groups about the C—H bonds renders such contacts structurally insignificant. In addition, we have discarded intermolecular C—H···O contacts in which the H···O distances exceed 2.50 Å and C—H···N contacts in which the H···N distances exceed 2.55 Å: these limits effectively exclude all the intermolecular contacts of C—H···O and C—H···N types. Finally, we have excluded from consideration the intermolecular C—H···Cl contacts in (VII), (X) and (XII), as it has been concluded that such contacts involving covalently bound Cl are probably no more than van der Waals contacts, and that geometrically they are certainly at the outer limit of what could conceivably be described as a hydrogen bond (Aakeröy *et al.*, 1999; Brammer *et al.*, 2001; Thallapally & Nangia, 2001).

**3.2.1. Finite (zero-dimensional) aggregation**. In (I) pairs of molecules are linked by paired N—H···N hydrogen bonds to form a cyclic centrosymmetric dimer characterized by an $R_2^2(8)$ (Bernstein *et al.*, 1995) motif (Fig. 2). This type of motif is the most important supramolecular building block in the present series and it is embedded in the hydrogen-bonded structures of (II)–(XI) as well as (I); indeed, of the compounds studied here, only in (XII) does an N—H···N hydrogen bond generate any motif other than a centrosymmetric $R_2^2(8)$ ring. Despite the presence of three independent N—H bonds in the molecule of (I), there are no direction-specific interactions between the $R_2^2(8)$ dimers. One N—H bond forms in the intramolecular N—H···O hydrogen bond, while the other N—H bond of the $NH_2$ group has no potential acceptor within hydrogen-bonding range, so the supramolecular aggregation is finite.

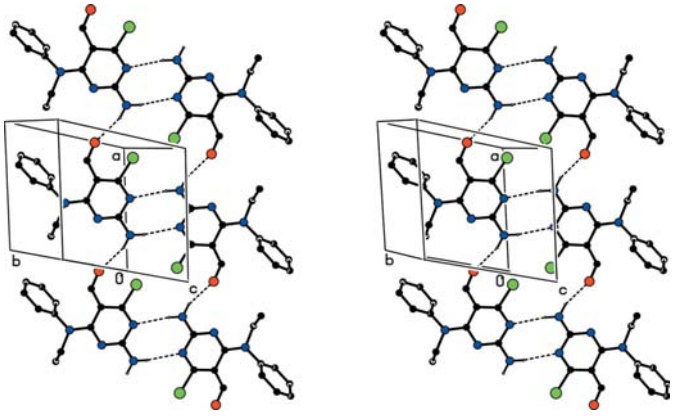

**Figure 4**
A stereoview of part of the crystal structure of (VI) showing the formation of a chain of edge-fused hydrogen-bonded $R_2^2(8)$ and $R_4^4(16)$ rings along [100]. For the sake of clarity the H atoms bonded to C atoms have been omitted.

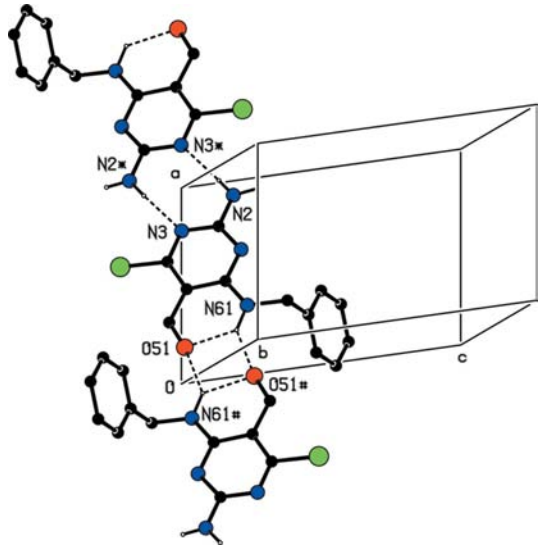


**Figure 5**
Part of the crystal structure of (VII) showing the formation of a chain of hydrogen-bonded $S(6)$, $R_2^2(4)$ and $R_2^2(8)$ rings along [2$\bar{1}$0]. For the sake of clarity the H atoms bonded to C atoms have been omitted. The atoms marked with an asterisk (*) or a hash (#) are at the symmetry positions $(2-x, -y, -z)$ and $(-x, 1-y, -z)$, respectively.

**3.2.2. One-dimensional aggregation**. The supramolecular aggregation in (II)–(V) is very similar, despite their different molecular constitutions and unit-cell dimensions, and only (II) need be described in any detail. In (II) the amino N2 atom in the molecule at $(x, y, z)$ acts as a hydrogen-bond donor, *via* H2*A*, to the O51 atom in the molecule at $(1-x, 1-y, 1-z)$, so forming by inversion an $R_2^2(16)$ ring centred at $(\frac{1}{2}, \frac{1}{2}, \frac{1}{2})$, while the same N2 atom acts as a donor, *via* H2*B*, to the N3 atom in the molecule at $(1-y, -y, 1-z)$, so forming the $R_2^2(8)$ ring characteristic of this series, centred at $(\frac{1}{2}, 0, \frac{1}{2})$. Propagation by inversion of these two hydrogen bonds then generates a chain of edge-fused rings running parallel to the [010] direction with the $R_2^2(8)$ rings centred at $(\frac{1}{2}, n, \frac{1}{2})$ (where $n$ represents zero or an integer) and the $R_2^2(16)$ rings centred at $(\frac{1}{2}, n+\frac{1}{2}, \frac{1}{2})$ (where $n$ represents zero or an integer) (Fig. 3). Entirely analogous chains of edge-fused rings are formed in (III)–(V), with the chains parallel to [010] in (III) and (IV), and parallel to [100] in (V). In none of (II)–(V) are there any direction-specific interactions between the chains. There are some C—H···(pyrimidine) contacts in (V), but since the pyrimidine rings are not classically aromatic, the structural significance of these contacts is probably minimal.

Compound (VI) contains the usual $R_2^2(8)$ motif generated by inversion, but the N—H···O hydrogen bonds link molecules related by translation. Propagation of the two hydrogen bonds by inversion and translation generates a chain of centrosymmetric edge-fused rings running parallel to the [100] direction with $R_2^2(8)$ rings centred at $(n, 0, \frac{1}{2})$ (where $n$ represents zero or an integer) and $R_4^4(16)$ rings centred at $(n+\frac{1}{2}, 0, \frac{1}{2})$ (where $n$ represents zero or an integer; Fig. 4).

The structure of (VII) contains the same $R_2^2(8)$ motif built from paired N—H···N hydrogen bonds between inversion-related molecules. In addition, a three-centre N—H···O2 hydrogen bond is present: one component of this system is intramolecular forming an $S(6)$ motif, while the other generates a centrosymmetric $R_2^2(4)$ motif. Propagation by inversion of these hydrogen bonds then generates a chain of rings running parallel to the $[2\bar{1}0]$ direction (Fig. 5). There are no direction-specific interactions between adjacent chains.

In (VIII) the formyl O atom plays no role in the supramolecular aggregation which depends on a combination of N—H···N and N—H···$\pi$(arene) hydrogen bonds. The amino N2 atom acts as a hydrogen-bond donor, *via* H2*B*, to the N3 atom in the molecule at $(2-x, 1-y, 1-z)$, so forming a centrosymmetric $R_2^2(8)$ motif, centred at $(1, \frac{1}{2}, \frac{1}{2})$: the same N2 atom also acts as a donor, this time *via* H2*A*, to the aryl ring (C61–C66) in the molecule at $(1-x, -y, 1-z)$, forming a second centrosymmetric motif centred at $(\frac{1}{2}, 0, \frac{1}{2})$. Propagation by inversion of these two interactions then generates a chain of edge-fused rings running parallel to the [110] direction, with the rings generated by the paired N—H···N hydrogen bonds centred at $(n, n-\frac{1}{2}, \frac{1}{2})$ (where $n$ represents zero or an integer), and the rings generated by the paired N—H···$\pi$(arene) hydrogen bonds centred at $(n+\frac{1}{2}, n, \frac{1}{2})$ (where $n$ represents zero or an integer; Fig. 6).

**3.2.3. Two-dimensional aggregation**. *$\pi$-Stacked hydrogen-bonded chains*: Two hydrogen bonds link the molecules of (IX) into a chain of centrosymmetric rings. The usual $R_2^2(8)$ motif of paired N—H···N hydrogen bonds generates a ring centred at $(1, \frac{1}{2}, \frac{1}{2})$; in addition, the phenyl C614 atom in the molecule at $(x, y, z)$ acts as a hydrogen-bond donor to the formyl O51 atom in the molecule at $(-x, 1-y, -z)$, so generating by inversion an $R_2^2(20)$ ring centred at $(0, \frac{1}{2}, 0)$. Propagation by inversion of these two hydrogen bonds then generates a chain of rings parallel to the [201] direction, in which $R_2^2(8)$ rings centred at $(2n-1, \frac{1}{2}, n-\frac{1}{2})$ (where $n$ represents zero or an integer) alternate with $R_2^2(20)$ rings centred at $(2n, \frac{1}{2}, n)$, (where $n$ represents zero or an integer; Fig. 7). These chains are weakly linked by a single $\pi\cdots\pi$

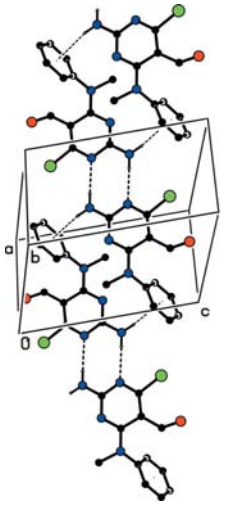

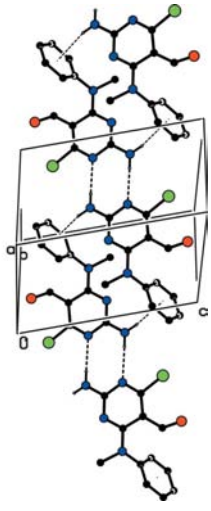

**Figure 6**
A stereoview of part of the crystal structure of (VIII) showing the formation of a chain of edge-fused centrosymmetric rings along [110]. For the sake of clarity the H atoms bonded to C atoms have been omitted.

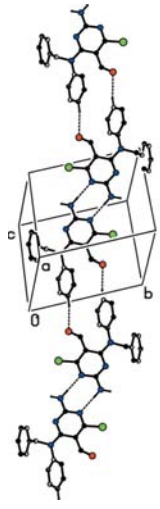

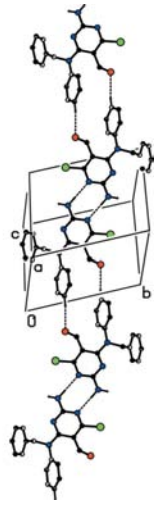

**Figure 7**
A stereoview of part of the crystal structure of (IX) showing the formation of a chain of edge-fused centrosymmetric rings along [201]. For the sake of clarity the H atoms bonded to C atoms and not involved in the motifs shown have been omitted.

stacking interaction to form sheets parallel to (010). The pyrimidine rings of the molecules at $(x, y, z)$ and $(1-x, 1-y, 1-z)$ are strictly parallel with an interplanar spacing of 3.438 (2) Å; the ring-centroid separation is 3.568 (2) Å and the ring-centroid offset is 0.954 (2) Å.

Hydrogen-bonded sheets: The hydrogen-bonded structures of (X) and (XI) are both two-dimensional, but their modes of construction are entirely different, depending upon two and three independent hydrogen bonds, respectively, although both structures contain $R_2^2(8)$ rings built from paired N—H···N hydrogen bonds (Table 3). The different modes of construction of the sheets reflect not only the additional donor and acceptor capacity available in (XI) by virtue of the presence of the hydroxyl group, but also the translational symmetry operators present in the structure of (X) but absent from that of (XI).

In (X) the amino N2 atom in the molecule at $(x, y, z)$, acts as a hydrogen-bond donor, *via* H2*B*, to the N3 atom in the molecule at $(1-x, 1-y, 1-z)$, so forming a dimeric $R_2^2(8)$ motif centred at $(\frac{1}{2}, \frac{1}{2}, \frac{1}{2})$. In addition, this atom also acts as a hydrogen-bond donor, *via* H2*A* to the formyl O atom in the molecule at $(\frac{1}{2}+x, \frac{1}{2}-y, \frac{1}{2}+z)$, so forming a $C(8)$ chain running parallel to the [101] direction and formed from molecules related by the *n*-glide plane at $y = 0.25$. The combination of the *n*-glide and inversion operations generates a sheet of alternating $R_2^2(8)$ and $R_6^6(32)$ rings parallel to $(10\bar{1})$ (Fig. 8). There are no direction-specific interactions between adjacent sheets.

The hydrogen-bonded structure of (XI), by contrast, depends on three independent centrosymmetric motifs, each formed by a single type of hydrogen bond. The amino N2 atom in the molecule at $(x, y, z)$ acts as a hydrogen-bond donor, *via* H2*A* and H2*B*, respectively, to the hydroxyl O64 atom in the molecule at $(1-x, 1-y, 1-z)$ and to the ring N3 atom in the molecule at $(3-x, -y, 1-z)$, so forming an $R_2^2(24)$ ring centred at $(\frac{1}{2}, \frac{1}{2}, \frac{1}{2})$ and an $R_2^2(8)$ ring centred at $(\frac{3}{2}\ 0, \frac{1}{2})$. In addition, the hydroxyl O64 atom at $(x, y, z)$ acts as a hydrogen-bond donor to the formyl O51 atom in the molecule at $(1-x, 1-y, -z)$, thus forming a second $R_2^2(24)$ ring, this time centred at $(\frac{1}{2}, \frac{1}{2}, 0)$. The combination of the $R_2^2(8)$ motif with each of the independent $R_2^2(24)$ motifs generates chains of fused rings running parallel to the $[2\bar{1}0]$ and $[2\bar{1}\bar{1}]$ directions, respectively, while the combination of the two $R_2^2(24)$ motifs generates a chain parallel to [001] (Fig. 9). The combination of any two of the chains along [001], $[2\bar{1}0]$ and $[2\bar{1}\bar{1}]$ generates a sheet parallel to (120).

**3.2.4. Three-dimensional aggregation**. There are only two hydrogen bonds in the structure of (XII), one each of N—H···O and N—H···N types (Table 3). Each of these hydrogen bonds acting alone generates a chain, while the combination of the two interactions acting alternately generates a third chain, such that the combination of all three chain motifs suffices to generate a three-dimensional framework structure.

In the first one-dimensional motif, the amino N2 atom in the molecule at $(x, y, z)$ acts as a hydrogen-bond donor, *via* H2*A*, to the carbonyl atom O51 in the molecule at $(-\frac{1}{2}+x, \frac{1}{2}-y, -\frac{1}{2}+z)$, so forming a $C(8)$ chain running parallel to the [101] direction and containing molecules related by the *n*-glide plane at $y = 0.25$ (Fig. 10*a*). In the second motif, the N2 atom at $(x, y, z)$ acts as a hydrogen-bond donor, this time *via* H2*B*, to the ring atom N1 in the molecule at $(x, 1-y, \frac{1}{2}+z)$, so forming a $C(4)$ chain running parallel to the [001] direction, containing molecules related by the *c*-glide plane at $y = \frac{1}{2}$ (Fig. 10*b*). Finally, the alternation of these two hydrogen bonds generates a $C_2^2(12)$ chain running parallel to the [110] direction (Fig. 10*c*), and the combination of chains along [001], [101] and [110] suffices to link all the molecules into a single hydrogen-bonded framework.

## 4. Concluding comments

The principal conclusions to be drawn from the present study are as follows:

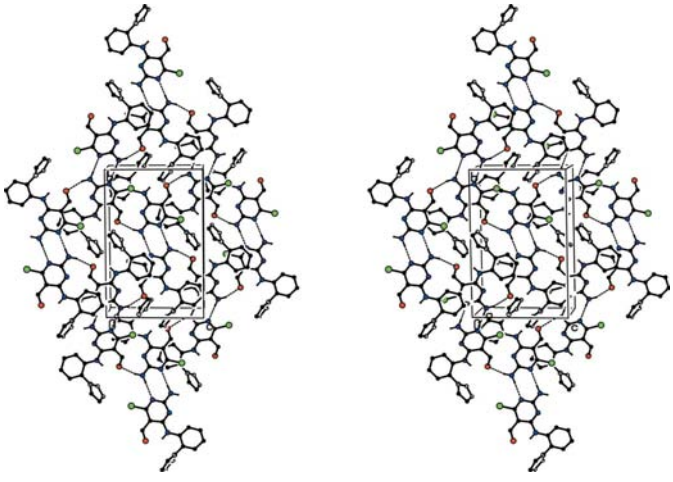

**Figure 8**
A stereoview of part of the crystal structure of (X) showing the formation of a hydrogen-bonded sheet parallel to $(10\bar{1})$ and built from alternating $R_2^2(8)$ and $R_6^6(32)$ rings. For the sake of clarity the H atoms bonded to C atoms have been omitted.

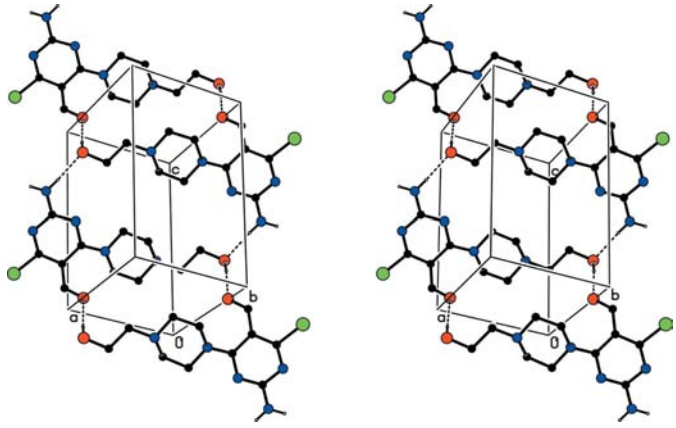

**Figure 9**
A stereoview of part of the crystal structure of (XI) showing the formation of a chain of edge-fused rings parallel to [001] and containing two types of $R_2^2(24)$ ring. For the sake of clarity the H atoms bonded to C atoms have been omitted.

(i) The presence of good electron-donor substituents and a good electron-acceptor substituent appropriately situated on a pyrimidine ring to generate a push–pull system leads to the development of strongly polarized, charge-separated electronic structures. This is manifested particularly in the similarity between the formally aromatic ring bond distances N1—C2 and N1—C6 on the one hand, and the formally single exocyclic bonds C2—N2 and C6—N61 on the other. It is also reflected in the restricted rotation of the amino groups about the C2—N2 bonds, as demonstrated by the solution NMR spectra. It is striking that these bond distances (Table 2) are almost identical in magnitude and pattern to the corresponding bond distances in the somewhat analogous 2,6-diamino-5-nitrosopyrimidines, exemplified by compounds such as *D* (Melguizo *et al.*, 2003) and *F* (Quesada *et al.*, 2004) (Scheme 1). Similarly, the elongation of the formyl C—O bond from its typical value in simple compounds is comparable in magnitude with the elongation of the N—O bond in the nitroso analogues. Against this, we note that the difference between the two ring C—C distances in (I)–(XII) reported here ranges from 0.033 (3) Å in (XII) to 0.050 (3) Å in (III), with a mean value of 0.043 (4) Å; by contrast, the corresponding difference in the 6-benzyloxy derivatives exemplified by *D* is consistently smaller, ranging from 0.009 (3) to 0.028 (4) Å, with a mean of 0.019 (4) Å, while in the triamino compounds exemplified by *F*, this difference is smaller still, ranging from zero to 0.013 (3) Å with a mean value of 0.006 (4) Å.

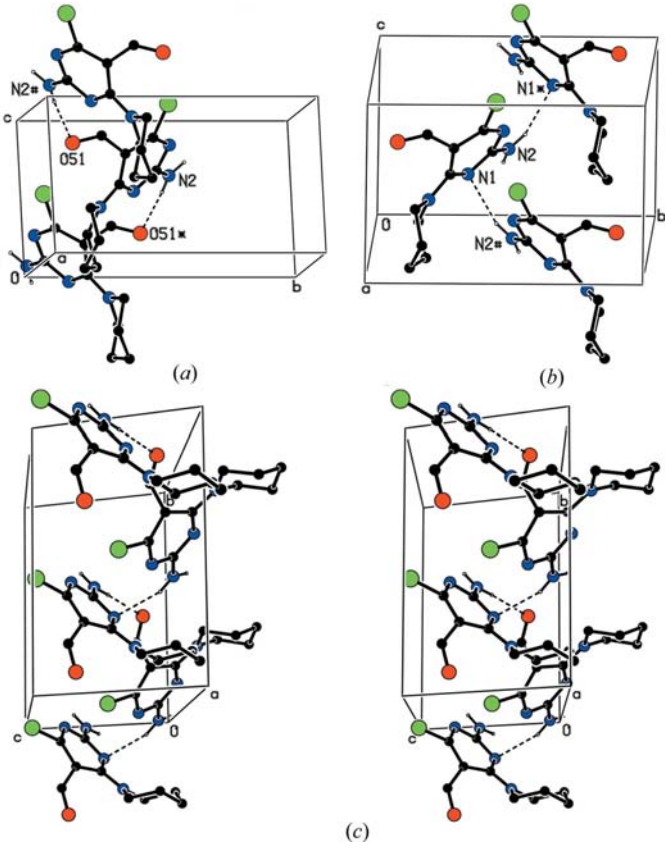


**Figure 10**
Parts of the crystal structure of (XII) showing the formation of three distinct chain motifs: (*a*) a *C*(8) chain parallel to [101], where the atoms marked with an asterisk (*) or a hash (#) are at the symmetry positions $(-\frac{1}{2}+x, \frac{1}{2}-y, -\frac{1}{2}+z)$ and $(\frac{1}{2}+x, \frac{1}{2}-y, \frac{1}{2}+z)$, respectively; (*b*) a *C*(4) chain parallel to [001], where the atoms marked with an asterisk (*) or a hash (#) are at the symmetry positions $(x, 1-y, \frac{1}{2}+z)$ and $(x, 1-y, -\frac{1}{2}+z)$, respectively; (*c*) a stereoview of a $C_2^2(12)$ chain parallel to [110]. In each case the H atoms bonded to C atoms have been omitted.

(ii) The development of polarized electronic structures appears to be independent of the puckering of the pyrimidine rings away from planarity, at least for the degree of puckering observed here, and in previous studies of nitro (Quesada *et al.*, 2003) and nitroso (Melguizo *et al.*, 2003; Quesada *et al.*, 2004) analogues. That distortions from fully coplanar geometry are possible without compromising significantly the electronic delocalization is confirmed by the observation that such delocalization occurs regardless of whether the formyl acceptor group is displaced from the mean plane of the ring atoms. Thus, for example, in (XII), where the displacements of atoms C51 and O51 are the largest in this series, the C—O bond is nonetheless the longest observed, at 1.233 (3) Å, while the four C—N bonds referred to in (i) above span a range of less than 0.01 Å. The ring puckering appears to arise from the presence of three adjacent substituents at the 4-, 5- and 6-positions of the pyrimidine ring, but it remains unclear at present why only some of the compounds in this study exhibit significant ring puckering, while the remainder contain planar pyrimidine rings. Thus, for example, although the three examples with planar rings, (I), (VII) and (X), all form intramolecular N—H···O hydrogen bonds, the other two, (VIII) and (IX), cannot do so. Again, (VIII) has a planar ring; (VI) with a slightly more bulky secondary amino substituent has a puckered ring; and (IX), where the secondary amino substituent is even more bulky, has a planar ring.

(iii) The patterns of intermolecular hydrogen bonding, and hence the crystal structures, are dominated by the formation, in 11 of the 12 structures reported here, of centrosymmetric $R_2^2(8)$ dimer motifs, formed by pairs of N—H···N hydrogen bonds and always involving the amino atom N2 as the donor and the pyrimidine ring atom N3 as the acceptor. These dimers are further linked by a range of other centrosymmetric motifs, including those of $R_2^2(4)$ type in (VII), $R_2^2(16)$ type in each of (II)–(V) and $R_2^2(20)$ type in (IX) and two types of $R_2^2(24)$ motif, based respectively on paired N—H···O and O—H···O hydrogen bonds, in (XI). A recent statistical survey (Eppel & Bernstein, 2008), based on structures retrieved from the Cambridge Structural Database (CSD; Allen, 2002), found that cyclic hydrogen-bonded motifs of this kind overwhelmingly lie across inversion centres. For the $R_2^2(8)$ motif involving paired N—H···N hydrogen bonds, motif **3** in Eppel & Bernstein (2008), which is the third most common of the $R_2^2(8)$ motifs identified after those based on pairs of N—H···O or O—H···O hydrogen bonds, some 69.6% of all occurrences involving achiral molecules and 90.4% of those involving racemic crystals had this motif lying across an inversion centre. For the $R_2^2(4)$ motif involving carbonyl O as the acceptor, motif **25** in Eppel & Bernstein (2008), which is actually a rather

uncommon motif found only with achiral molecules, just over half (55.8%) of structures had this motif lying across an inversion centre. The other motifs observed in the present study were not analysed by Eppel & Bernstein (2008). It is by no means obvious why centrosymmetric hydrogen-bonded motifs should be wholly absent from the crystal structure of compound (XII), when two such motifs are present in the crystal structure of the closely similar compound (III).

X-ray data were collected at Servicios Técnicos de Investigación, Universidad de Jaén, Spain. JC, AM and MN thank the Consejería de Innovación, Ciencia y Empresa (Junta de Andalucía, Spain) and the Universidad de Jaén for financial support. JT and JQ thank COLCIENCIAS and UNIVALLE (Universidad del Valle, Colombia) for financial support and for supporting a short research visit by JT to Departamento de Química Inorgánica y Orgánica, Universidad de Jaén.

## References

Aakeröy, C. B., Evans, T. A., Seddon, K. R. & Pálinkó, I. (1999). *New J. Chem.* pp. 145–152.
Allen, F. H. (2002). *Acta Cryst.* B**58**, 380–388.
Allen, F. H., Kennard, O., Watson, D. G., Brammer, L., Orpen, A. G. & Taylor, R. (1987). *J. Chem. Soc. Perkin Trans. 2*, pp. S1–S19.
Bernstein, J., Davis, R., Shimoni, L. & Chang, N.-L. (1995). *Angew. Chem. Int. Ed. Engl.* **34**, 1555–1573.
Brammer, L., Bruton, E. A. & Sherwood, P. (2001). *Cryst. Growth Des.* **1**, 277–290.
Burla, M. C., Caliandro, R., Camalli, M., Carrozzini, B., Cascarano, G. L., De Caro, L., Giacovazzo, C., Polidori, G. & Spagna, R. (2005). *J. Appl. Cryst.* **38**, 381–388.
Chae, M. Y., McDougall, M. G., Dolan, M. E., Swenn, K., Pegg, A. E. & Moschel, R. C. (1995). *J. Med. Chem.* **38**, 359–365.
Cremer, D. & Pople, J. A. (1975). *J. Am. Chem. Soc.* **97**, 1354–1358.
Duisenberg, A. J. M., Hooft, R. W. W., Schreurs, A. M. M. & Kroon, J. (2000). *J. Appl. Cryst.* **33**, 893–898.
Duisenberg, A. J. M., Kroon-Batenburg, L. M. J. & Schreurs, A. M. M. (2003). *J. Appl. Cryst.* **36**, 220–229.
Eppel, S. & Bernstein, J. (2008). *Acta Cryst.* B**64**, 50–56.
Ferguson, G. (1999). *PRPKAPPA*. University of Guelph, Canada.
Flack, H. D. (1983). *Acta Cryst.* A**39**, 876–881.
Friedman, H. S. *et al.* (1998). *J. Clin. Oncol.* **16**, 3570–3575.
Hooft, R. W. W. (1999). *COLLECT*. Nonius BV, Delft, The Netherlands.
Low, J. N., Ferguson, G., López, R., Arranz, P., Cobo, J., Melguizo, M., Nogueras, M. & Sánchez, A. (1997). *Acta Cryst.* C**53**, 890–892.
Low, J. N., Godino, M. L., López, R., Pérez, A., Melguizo, M. & Cobo, J. (1999). *Acta Cryst.* C**55**, 1727–1730.
Low, J. N., Howie, R. A., Hueso-Ureña, F. & Moreno-Carretero, M. N. (1992). *Acta Cryst.* C**48**, 145–147.
Low, J. N., López, M. D., Arranz Mascarós, P., Cobo Domingo, J., Godino, M. L., López Garzón, R., Gutiérrez, M. D., Melguizo, M., Ferguson, G. & Glidewell, C. (2000). *Acta Cryst.* B**56**, 882–892.
Low, J. N., Trilleras, J., Cobo, J., Marchal, A. & Glidewell, C. (2007). *Acta Cryst.* C**63**, o681–o684.
McArdle, P. (2003). *OSCAIL for Windows*, Version 10. Crystallography Centre, Chemistry Department, NUI Galway, Ireland.
Melguizo, M., Quesada, A., Low, J. N. & Glidewell, C. (2003). *Acta Cryst.* B**59**, 263–276.
Otwinowski, Z. & Minor, W (1997). *Methods in Enzymology*, Vol. 276, *Macromolecular Crystallography*, edited by C. W. Carter Jr & R. M. Sweet, Part A, pp. 307–326. New York: Academic Press.
Portalone, G. & Colapietro, M. (2007). *Acta Cryst.* C**63**, o650–o654.
Quesada, A., Marchal, A., Low, J. N. & Glidewell, C. (2003). *Acta Cryst.* C**59**, o102–o104.
Quesada, A., Marchal, A., Melguizo, M., Low, J. N. & Glidewell, C. (2004). *Acta Cryst.* B**60**, 76–89.
Quesada, A., Marchal, A., Melguizo, M., Nogueras, M., Sánchez, A., Low, J. N., Cannon, D., Farrell, D. M. M. & Glidewell, C. (2002). *Acta Cryst.* B**58**, 300–315.
Quiroga, J., Trilleras, J., Insuasty, B., Abonía, R., Nogueras, M., Marchal, A. & Cobo, J. (2008). *Tetrahedron Lett.* **49**, 3257–3259.
Riddell, F. & Rogerson, M. (1996). *J. Chem. Soc. Perkin Trans. 2*, pp. 493–504.
Riddell, F. & Rogerson, M. (1997). *J. Chem. Soc. Perkin Trans. 2*, pp. 249–255.
Seela, F. & Sterker, H. (1986). *Helv. Chim. Acta*, **69**, 1602–1613.
Sheldrick, G. M. (2003). *SADABS*, Version 2.10. University of Göttingen, Germany.
Sheldrick, G. M. (2008). *Acta Cryst.* A**64**, 112–122.
Spek, A. L. (2003). *J. Appl. Cryst.* **36**, 7–13.
Taylor, E. C. & Gillespie, P. (1992). *J. Org. Chem.* **57**, 5757–5761.
Thallapally, P. K. & Nangia, A. (2001). *CrystEngComm*, **27**, 1–6.
Torre, J. M. de la, Nogueras, M., Cobo, J., Low, J. N. & Glidewell, C. (2007). *Acta Cryst.* C**63**, o638–o640.
Trilleras, J., Quiroga, J., Low, J. N., Cobo, J. & Glidewell, C. (2007). *Acta Cryst.* C**63**, o758–o760.
Wilson, A. J. C. (1976). *Acta Cryst.* A**32**, 994–996.